

1 **Wild-type U2AF1 antagonizes the splicing program characteristic of U2AF1-**  
2 **mutant tumors and is required for cell survival**

3

4

5 Short title: Interplay of mutant and wild-type U2AF1

6

7

8 Dennis Liang Fei<sup>1,2,\*</sup>, Hayley Motowski<sup>1</sup>, Rakesh Chatrikhi<sup>3</sup>, Sameer Prasad<sup>1</sup>, Jovian  
9 Yu<sup>1</sup>, Shaojian Gao<sup>4</sup>, Clara L. Kielkopf<sup>3,\*</sup>, Robert K. Bradley<sup>5,6,\*</sup>, Harold Varmus<sup>1,2\*</sup>

10

11

12 1. Cancer Biology Section, Cancer Genetics Branch, National Human Genome  
13 Research Institute, Bethesda, MD 20892, United States

14 2. Department of Medicine, Meyer Cancer Center, Weill Cornell Medicine, New York,  
15 NY 10065, United States

16 3. Department of Biochemistry and Biophysics, Center for RNA Biology, University of  
17 Rochester Medical Center, Rochester, NY 14642, United States

18 4. Genetics Branch, National Cancer Institute, Bethesda, Maryland, 20892, United  
19 States

20 5. Computational Biology Program, Public Health Sciences Division, Fred Hutchinson  
21 Cancer Research Center, Seattle, WA 98109, United States

22 6. Basic Sciences Division, Fred Hutchinson Cancer Research Center, Seattle,  
23 Washington 98109, United States

24

25

26 \* Correspondence: D.L.F. [dlf2002@med.cornell.edu](mailto:dlf2002@med.cornell.edu); C.L.K.

27 [clara\\_kielkopf@urmc.rochester.edu](mailto:clara_kielkopf@urmc.rochester.edu); R.K.B. [rbradley@fredhutch.org](mailto:rbradley@fredhutch.org); H.V.

28 [varmus@med.cornell.edu](mailto:varmus@med.cornell.edu)

29

30

31 Keywords: U2AF1, splicing factor, S34F, RNA binding, lung adenocarcinoma

32 **Abstract**

33           We have asked how the common S34F mutation in the splicing factor U2AF1  
34 regulates alternative splicing in lung cancer, and why wild-type U2AF1 is retained in  
35 cancers with this mutation. A human lung epithelial cell line was genetically modified so  
36 that *U2AF1S34F* is expressed from one of the two endogenous *U2AF1* loci. By altering  
37 levels of mutant or wild-type U2AF1 in this cell line and by analyzing published data on  
38 human lung adenocarcinomas, we show that S34F-associated changes in alternative  
39 splicing are proportional to the ratio of S34F:wild-type gene products and not to  
40 absolute levels of either the mutant or wild-type factor. Preferential recognition of  
41 specific 3' splice sites in S34F-expressing cells is largely explained by differential *in vitro*  
42 RNA-binding affinities of mutant versus wild-type U2AF1 for those same 3' splice sites.  
43 Finally, we show that lung adenocarcinoma cell lines bearing *U2AF1* mutations do not  
44 require the mutant protein for growth *in vitro* or *in vivo*. In contrast, wild-type U2AF1 is  
45 required for survival, regardless of whether cells carry the *U2AF1S34F* allele. Our  
46 results provide mechanistic explanations of the magnitude of splicing changes observed  
47 in *U2AF1*-mutant cells and why tumors harboring *U2AF1* mutations always retain an  
48 expressed copy of the wild-type allele.

49

50

## 51 **Author Summary**

52           Large-scale genomics studies have identified recurrent mutations in many genes  
53 that fall outside the conventional domain of proto-oncogenes. They include genes  
54 encoding factors that mediate RNA splicing; mutations affecting four of these genes are  
55 present in up to half of proliferative myeloid disorders and in a significant number of  
56 solid tumors, including lung adenocarcinoma. Here we have characterized several  
57 properties of a common mutant version of the U2AF1 splicing factor, a component of  
58 the U2 auxiliary factor complex, in lung cells. We have found that mutant-associated  
59 changes in splice site selection are primarily influenced by the ratio of mutant and wild-  
60 type U2AF1 gene products; thus increasing wild-type U2AF1 levels represses the  
61 mutant-induced splicing program. We show that the altered splice site preferences of  
62 mutant U2AF1 can be attributed to changes in its binding to relevant 3' splice sites. We  
63 also show that mutant U2AF1 is different from some oncogenes: the growth properties  
64 of lung cancer cell lines carrying the mutant allele are unaffected by loss of the mutant  
65 gene, while the wild-type allele is absolutely required for survival. These results  
66 advance our understanding of the molecular determinants of the mutant-associated  
67 splicing program, and they highlight previously unappreciated roles of wild-type U2AF1  
68 in the presence of the recurrent *U2AF1*S34F mutation.

69 **Introduction**

70 Somatic mutations in genes encoding four splicing factors (*U2AF1*, *SF3B1*,  
71 *SRSF2* and *ZRSR2*) have recently been reported in up to 50% of myelodysplastic  
72 syndromes (MDS) and related neoplasms and at lower frequencies in a variety of solid  
73 tumors [1-9]. Among these factors, only *U2AF1* is known to be recurrently mutated in  
74 lung adenocarcinomas (LUADs) [3,9]. The only recurrent missense mutation of *U2AF1*  
75 in LUAD affects codon 34 and always changes the conserved serine in a zinc knuckle  
76 motif to phenylalanine (p.Ser34Phe, or S34F). This striking mutational consistency  
77 suggests a critical, yet unknown, role for *U2AF1*S34F during lung carcinogenesis. In  
78 addition, the wild-type (WT) *U2AF1* allele is always retained in cancers with common  
79 *U2AF1* mutations, including *U2AF1*S34F [2]. However, the functional significance of the  
80 wild-type allele in cells with mutant *U2AF1* is not known.

81 *U2AF1* is a component of the U2 small nuclear ribonucleoprotein auxiliary factor  
82 complex (U2AF) [10,11]. During early spliceosome assembly, U2AF recognizes  
83 sequences at the 3' ends of introns to facilitate the recruitment of the U2 small nuclear  
84 ribonucleoprotein (snRNP) complex to the 3' splice site; the recruitment occurs in  
85 conjunction with recognition of the intronic branch point by splicing factor 1 (SF1)  
86 [12,13]. *In vitro* crosslinking assays showed that *U2AF1* contacts the AG dinucleotide at  
87 the intron-exon boundary and flanking sequences [14-16].

88 Consistent with the critical role that *U2AF1* plays in RNA splicing, *U2AF1*  
89 mutations are known to cause specific alterations in RNA splicing, most notably  
90 affecting the inclusion of cassette exons in mRNA [17-20]. However, the precise  
91 molecular basis of these splicing alterations, as well as how they are quantitatively

92 regulated, is unknown. One possibility is that U2AF1 mutations cause altered RNA-  
93 binding affinity, resulting in altered splice site recognition. A computational model of the  
94 structure of the U2AF1:RNA complex suggested that Ser34 is a critical residue that  
95 contacts RNA [17]. Another study reported that U2AF1S34F exhibited altered affinity  
96 relative to the wild-type protein for RNA oligonucleotides derived from a cassette exon  
97 whose recognition is repressed in S34F-expressing cells [18]. Finally, the S34F  
98 mutation reportedly prevented a minimal fission yeast U2AF heterodimer from binding to  
99 a particular 3' splice site RNA sequence [21]. However, it is not known whether altered  
100 RNA binding accounts for most S34F-associated splicing alterations and whether  
101 mechanisms other than altered binding control S34F-associated splicing.

102         Here, we combine genetic and biochemical approaches to show that wild-type  
103 U2AF1 antagonizes the S34F-associated splicing program in lung epithelial cells.  
104 Analyses of the transcriptomes of primary LUAD samples as well as isogenic lung cells  
105 in culture indicate that the ratio of mutant to wild-type U2AF1 gene products is a critical  
106 determinant of the magnitude of S34F-associated changes in alternative splicing. S34F-  
107 associated splicing alterations can be largely explained by differences in the relative  
108 affinities of U2AF-SF1 complexes containing mutant versus wild-type U2AF1 for RNA  
109 containing the relevant 3' splice sites. Moreover, we show that proliferation of cancer  
110 cells with *U2AF1S34F* is critically dependent on expression of the wild-type, but not the  
111 mutant, allele of *U2AF1*.

112

## 113 **Results**

### 114 **S34F-associated splicing correlated with S34F:WT mRNA ratios in LUAD**

115 Before undertaking experiments to study the effects of mutant U2AF1 in cultured  
116 cells, we first examined 512 transcriptomes from primary human LUADs published by  
117 The Cancer Genome Atlas (TCGA) [9]. Thirteen of these tumors harbor the most  
118 common *U2AF1* mutation, S34F. (Two others carry rare mutations of unknown  
119 significance, S65L and G216R, and were not considered further.) We identified cassette  
120 exons whose inclusion was increased or decreased by ten percent or more in each  
121 tumor with the S34F mutation relative to the median inclusion of each cassette exon  
122 across all tumors without a *U2AF1* mutation. We then identified consensus sequence  
123 motifs for the 3' splice sites lying immediately upstream of the cassette exons that were  
124 promoted or repressed in association with *U2AF1*S34F, represented by “sequence  
125 logos” as shown in Figs. 1A and S1. The same analysis was performed on 19 random  
126 tumors lacking a *U2AF1* mutation as controls.

127 As illustrated by data from patient 7903 in Fig. 1A, over two hundred cassette  
128 exons were included more frequently and a similar number were included less  
129 frequently in this *U2AF1*-mutant tumor. Notably, as illustrated by the sequence logos,  
130 the nucleotide distribution at the -3 position (boxed) of promoted and repressed exons  
131 was different from that observed upstream of the much larger number of unaffected  
132 exons: A replaced T as the second most common nucleotide preceding the promoted  
133 exons, while T was more common than C in the sequence preceding the repressed  
134 exons. These patterns were observed in nine of the thirteen tumors with the  
135 *U2AF1*S34F allele (Supplemental Fig. S1A). They have been observed previously in

136 comparisons between transcriptomes carrying the *U2AF1*S34F allele with wild-type  
137 transcriptomes [17-20], and are therefore henceforth referred to as the “typical S34F”  
138 consensus 3' splice sites. In the other four tumors with the *U2AF1*S34F mutation, these  
139 “typical S34F” consensus 3' splice sites were partially or completely absent (Figs. 1A,  
140 S1B). Those four tumors exhibited consensus 3' splice sites that were similar to the  
141 consensus 3' splice sites identified in tumors lacking a *U2AF1* mutation, where  
142 variations in inclusion relative to the median wild-type sample are presumably stochastic  
143 (Supplemental Fig. S1C). Thus, we henceforth refer to these sequence patterns, as  
144 shown for tumor from patient 7727 in Fig. 1A, as “quasi-WT”.

145 To explain why transcriptomes of some tumors with *U2AF1* mutations showed a  
146 typical S34F-associated consensus 3' splice sites, while others exhibited quasi-WT  
147 patterns, we estimated the levels of mutant and total *U2AF1* mRNA based on available  
148 data from the tumors to determine the ratio of mutant to wild-type (S34F:WT) mRNA.  
149 Tumors with quasi-WT patterns had low S34F:WT mRNA ratios (ranging from 0.27 to  
150 0.31), whereas all but one tumor with the S34F-associated pattern had higher ratios  
151 (0.43 or more) (Fig. 1B). In contrast, absolute levels of *U2AF1*S34F mRNA or total  
152 *U2AF1* mRNA levels were not different between these two groups of tumors  
153 (Supplemental Figs. S2A, B).

154 We next sought to understand the origin of the wide range of S34F:WT ratios that  
155 we observed. These ratios, ranging from 0.26 to 0.82, could not be explained by  
156 contamination of tumor cells with non-tumor cells, since the proportion of tumor nuclei  
157 reported for these samples did not correlate with S34F:WT mRNA ratios (Fig. 1C) or  
158 with the presence or absence of the expected S34F-associated consensus 3' splice

159 sites (Supplemental Fig. S2C). Conversely, *U2AF1* DNA copy number correlated with  
160 the estimated levels of total *U2AF1* mRNA (Supplemental Fig. S2D). Seven of the 13  
161 *U2AF1*S34F mutant samples, including two of the four samples displaying quasi-WT  
162 consensus 3' splice site sequences, showed either copy number loss or gain at the  
163 *U2AF1* locus, suggesting that copy number variation (CNV) might account, at least in  
164 part, for the varying S34F:WT mRNA ratios in LUAD samples (Fig. 1B). Unbalanced  
165 allelic expression or proportions of tumor subclones might also contribute to the variable  
166 S34F:WT mRNA ratios, although these possibilities could not be readily tested using the  
167 available LUAD data.

168 We next tested whether the *U2AF1* S34F:WT ratio was associated with  
169 quantitative changes in splicing (versus the qualitative differences in consensus 3' splice  
170 sites described above). We correlated S34F:WT ratios with the quantitative inclusion of  
171 specific S34F-responsive cassette exons and 5' extensions of exons resulting from  
172 competing 3' splice sites that were reported previously [17,19,20]. We studied three  
173 cassette exons that exhibited less (*ASUN* and *STRAP*) or more (*ATR*) inclusion, and  
174 two 5' extensions of exons (*FMR1* and *CASP8*) that were used less frequently in the  
175 presence of *U2AF1*S34F. Tumors with the highest S34F:WT mRNA ratios showed the  
176 lowest inclusion levels of the cassette exon in *STRAP* mRNA, whereas tumors without a  
177 *U2AF1* mutation had the highest level of inclusion (Fig. 1D; Pearson correlation of -  
178 0.79). Similar correlations were observed between inclusion levels of other  
179 representative exons and S34F:WT mRNA ratios (Supplemental Fig. S3, panels E, I, M  
180 and Q). As controls, we tested for correlations between the inclusion of these cassette  
181 exons and levels of *U2AF1*S34F mRNA, total *U2AF1* mRNA, or percent tumor nuclei.

182 None of these analyses, with the exception of the *U2AF1*S34F mRNA level versus the  
183 inclusion of the 5' extension of the *FMR1* exon, showed a relationship as strong as that  
184 observed for the S34F:WT mRNA ratio (Supplemental Figs. S3 panels B-D, F-H, J-L, N-  
185 P and R-T). These results indicate that the S34F:WT mRNA ratio predicts the  
186 magnitude of S34F-associated splicing in human LUAD.

187

### 188 **Creation of isogenic lung cell lines that recapitulated features of S34F-associated** 189 **splicing in LUAD.**

190 The results presented in the preceding section, based on analyses of LUAD  
191 tumors with the *U2AF1*S34F mutation, suggest that the magnitude of S34F-associated  
192 splicing is a function of the S34F:WT mRNA ratio. To directly test this hypothesis, we  
193 developed a cell line that allows manipulation of WT and mutant U2AF1 gene product  
194 levels and measurement of the corresponding effects on RNA splicing.

195 The human bronchial epithelial cell line (HBEC3kt) was previously derived from  
196 normal human bronchial tissue and immortalized by introduction of expression vectors  
197 encoding human telomerase reverse transcriptase (*hTERT*) and cyclin-dependent  
198 kinase-4 (*CDK4*) [22]. To knock in a *U2AF1*S34F allele at an endogenous locus in  
199 HBEC3kt cells, we adopted a published genomic DNA editing approach [23], using the  
200 *PiggyBac* transposon that leaves no traces of exogenous DNA at the locus (Fig. 2A; see  
201 Supplemental Materials and Methods for details). We identified three cell clones at  
202 intermediate stages of gene editing after screening more than 50 primary transfectants  
203 (Supplemental Fig. S4A, B). Sanger sequencing of these intermediate clones revealed  
204 that one of the three clones carried the desired S34F missense sequence, while two

205 clones were wild-type (Supplemental Fig. S4C). Wild-type intermediates are expected  
206 because a homologous sequence between the S34F point mutation and the drug  
207 cassette in the vector can serve as the 5' homology arm for recombination (designated  
208 as 5' HA#2 in Fig. 2A). From the final clones derived from these intermediates (after  
209 transposition to remove the drug cassette flanked by the *PiggyBac* elements), we chose  
210 one subclone from each of the two wild-type intermediate clones (referred to as WT1  
211 and WT2 cells) and two subclones from the sole mutant intermediate clone (referred to  
212 as MUT1a and MUT1b cells) for all subsequent experiments with isogenic HBEC3kt  
213 cells (Supplemental Fig. S4D). The MUT and WT cells all expressed similar levels of  
214 *U2AF1* mRNA and protein (Supplemental Fig. S4E). Using high-throughput mRNA  
215 sequencing (RNA-seq) and allele-specific RT-qPCR, we observed similar levels of wild-  
216 type and mutant *U2AF1* mRNAs in the MUT cells (Figs. 2B, S5C), consistent with  
217 heterozygosity at the *U2AF1* locus.

218 To determine how the engineered *U2AF1* S34F allele affects mRNA splicing, we  
219 first assayed the inclusion levels of 20 cassette exons that were previously reported to  
220 be associated with mutant *U2AF1* in both LUAD and AML (acute myeloid leukemia)  
221 [19]. We confirmed that all 20 of these cassette exons, which included the previously  
222 studies *ASUN* and *STRAP* cassette exons, were indeed S34F-dependent in our  
223 engineered cells using RT-qPCR with isoform-specific primers (Figs. 2C, S6).

224 We next evaluated the global difference in cassette exon recognition in MUT  
225 versus WT cells using RNA-seq (Supplemental Table S1). MUT and WT cells were  
226 grouped separately in an unsupervised cluster analysis based on cassette exon  
227 inclusion (Fig. 2D). We observed the expected consensus 3' splice sites of cassette

228 exons that were promoted or repressed in MUT versus WT cells (Fig. 2E). Overall,  
229 these results indicate that we successfully created clonal HBEC3kt cells isogenic for  
230 *U2AF1S34F* and that the MUT cells exhibited similar alterations in splicing relative to  
231 their WT counterparts as do primary LUAD transcriptomes.

232

233 **The ratio of S34F:WT gene products controlled S34F-associated splicing in**  
234 **isogenic lung cells.**

235 We next used our isogenic cell model with the *U2AF1S34F* mutation to test the  
236 hypothesis that the S34F:WT ratio, rather than absolute levels of the mutant or wild-type  
237 gene products, controls S34F-associated splicing. We tested two specific predictions.  
238 First, changing the levels of *U2AF1S34F* while keeping the S34F:WT ratio constant  
239 should not affect S34F-associated splicing. Second, changing the level of wild-type  
240 *U2AF1* while keeping the level of *U2AF1S34F* constant (e.g., allowing the S34F:WT  
241 ratio to change) should alter the inclusion of S34F-dependent cassette exons. We  
242 tested these predictions in the isogenic HBEC3kt cells by manipulating levels of wild-  
243 type or mutant *U2AF1* gene products and measuring the subsequent changes in S34F-  
244 associated splicing.

245 We first reduced the amounts of both mutant and wild-type *U2AF1* mRNA  
246 concordantly in MUT1a cells, keeping the S34F:WT mRNA ratio constant. This was  
247 achieved by transducing MUT1a cells with short hairpin RNAs (shRNAs) that target  
248 regions of the *U2AF1* transcripts distant from the S34F missense mutation. The same  
249 shRNAs were also introduced in WT1 cells as a control. Allele-sensitive RT-qPCR  
250 confirmed that the mRNA ratio of the mutant and wild-type *U2AF1* remained constant

251 (Supplemental Fig. S7A), while the overall U2AF1 mRNA and protein levels were  
252 reduced by more than 90% (Figs. 3A, bottom panel, and S7B). Knockdown of total  
253 *U2AF1* in both MUT1a and WT1 cells did not cause significant changes in recognition of  
254 the *ASUN* or *STRAP* cassette exons, two splicing events that are strongly associated  
255 with *U2AF1*S34F, in either cell line (Fig. 3A, upper panels). Similar results were  
256 obtained for two additional S34F-associated cassette exons in *USP25* and *AXL* that  
257 exhibit increased inclusion in cells expressing *U2AF1*S34F (Supplemental Fig. S7C, D).

258 We next confirmed that knockdown of *U2AF1* was sufficient to alter splicing  
259 events known to be dependent on wild-type U2AF1. We studied a competing 3' splice  
260 site event in *SLC35C2*, in which the use of an intron-proximal over an intron-distal 3'  
261 splice site depends on the level of U2AF1 independent of a *U2AF1* mutation [24].  
262 Knockdown of total *U2AF1* in either WT1 or MUT1a cell lines reduced the use of the  
263 U2AF1-dependent intron-proximal 3' splice site (Supplemental Fig. S7E). Thus,  
264 reduction of *U2AF1* to levels sufficient to affect U2AF1-dependent alternative splicing  
265 did not affect S34F-associated splicing in MUT1a cells when the S34F:WT ratio was  
266 maintained.

267 We next altered the S34F:WT ratio by separately overexpressing mutant or wild-  
268 type *U2AF1* in WT1 and MUT1a cells and examining the subsequent changes in the  
269 recognition of the *ASUN* and *STRAP* cassette exons. These cassette exons are  
270 preferentially excluded in cells expressing *U2AF1*S34F. Increasing the amount of  
271 U2AF1S34F protein—hence increasing the S34F:WT ratio in either cell type—further  
272 enhanced skipping of these cassette exons (Fig. 3B). Conversely, decreasing the  
273 S34F:WT ratio in MUT1a cells by increasing the production of wild-type U2AF1 protein

274 reduced the extent of exon skipping to approximately the same levels seen in WT1 cells  
275 (Fig. 3B).

276 We also altered the production of wild-type U2AF1 mRNA and protein in MUT1a  
277 cells by disrupting the endogenous wild-type *U2AF1* locus with the CRISPR-Cas9  
278 system. Single-guide RNAs (sgRNAs) designed to match either the WT or mutant  
279 *U2AF1* sequences were shown to disrupt either reading frame selectively, generating  
280 indels (insertions and deletions) at the *U2AF1* locus and thereby changing the S34F:WT  
281 ratios (Supplemental Figs. S8, S9). Since WT *U2AF1* is required for the growth of these  
282 cells (as shown below; Fig. 6), we extracted RNA and protein from cells six days after  
283 transduction with Cas9 and sgRNA-WT, when depletion of wild-type U2AF1 was  
284 incomplete (Fig. 3C). Selective disruption of wild-type *U2AF1* increased the S34F:WT  
285 mRNA ratio in MUT1a cells; as predicted, the extent of exon skipping was further  
286 increased in *ASUN* and *STRAP* mRNAs (Fig. 3C). Notably, the degree of exon skipping  
287 induced by mutant cDNA was similar to that caused by disrupting the wild-type *U2AF1*  
288 allele (compare Figs. 3C with 3B), even though the absolute protein levels of  
289 U2AF1S34F were different in the two experiments. These results show that wild-type  
290 U2AF1 antagonizes the activity of U2AF1S34F by a competitive mechanism, such that  
291 the S34F:WT ratio controls the magnitude of S34F-associated splicing changes  
292 independent of levels of either mutant or wild-type protein.

293

#### 294 **Disruption of WT U2AF1 globally enhanced S34F-associated splicing.**

295 Results in the preceding sections are based on studies of a few well-documented  
296 S34F-responsive cassette exons that likely serve as surrogates for the global effects of

297 U2AF1S34F on splice site recognition. To determine whether these results reflect  
298 general rules governing S34F-associated splicing, we used RNA-seq to measure the  
299 consequences of altering S34F:WT ratios on global recognition of cassette exons.  
300 When wild-type *U2AF1* was diminished by CRISPR-Cas9-mediated disruption in  
301 MUT1a cells (see Fig. 3C), the S34F-associated changes in inclusion (Fig. 4A) or  
302 exclusion (Fig. 4B) of cassette exons were enhanced. These global effects are  
303 consistent with our measurements of individual cassette exons by RT-qPCR (Fig. 3C).  
304 An unsupervised cluster analysis suggests that disruption of wild-type *U2AF1* in MUT1a  
305 cells primarily enhances the magnitude of changes for S34F-associated cassette exons  
306 (Fig. 4C). We also observed a modest increase in the preference for C versus T at the -  
307 3 position of the consensus 3' splice sites of cassette exons that were promoted versus  
308 repressed in association with *U2AF1*S34F (Fig. 4D) following reduction of wild-type  
309 *U2AF1* levels, consistent with the observed association between the S34F:WT mRNA  
310 ratio and typical S34F-associated consensus 3' splice sites identified in LUAD tumor  
311 transcriptomes (Fig. 1).

312 We observed similar results when we extended our analyses to include other  
313 types of alternative splicing beyond cassette exon recognition (Supplemental Fig. S10).  
314 We used RT-qPCR to validate five splicing alterations that are sensitive to ablation of  
315 wild-type *U2AF1* in the presence of *U2AF1*S34F (Supplemental Fig. S11). Two of the  
316 five events involve incorporation of cassette exons (in *ATR* and *MED15*), two involve  
317 competition between different 3' splice sites (in *CASP8* and *SRP19*), and one involves a  
318 choice between two mutually exclusive exons (in *H2AFY*). We conclude that the

319 importance of the S34F:WT ratio for S34F-dependent splicing changes extends from  
320 cassette exon recognition to other types of alternative splicing.

321

322 **Changes in RNA splicing correlated with relative binding affinities of mutant and**  
323 **WT U2AF1 complexes.**

324         Based on the role of U2AF1 in 3' splice site recognition, we hypothesized that  
325 differential RNA binding by mutant and WT U2AF1 could contribute to the observed  
326 dependence of S34F-associated splicing on the WT:S34F ratios. It has previously been  
327 shown that the S34F mutation reduces the binding affinity of the U2AF1-containing  
328 complex for a representative skipped splice site [18]. However, whether changes in  
329 RNA binding could account for exon inclusion, as well as the generality of this  
330 observation, were unknown. We therefore tested whether altered RNA-binding affinity  
331 could explain mutation-dependent increases (*ZFAND1*, *FXR1*, *ATR*, *MED15*) and  
332 decrease (*CEP164*) in exon inclusion, as well as competing 3' splice site recognition  
333 (*FMR1*). These splicing events exhibited S34F-associated alterations in both our  
334 isogenic cell lines (Supplemental Table S1) and in LUAD transcriptomes (Supplemental  
335 Table S2).

336         We determined the RNA binding affinities of purified U2AF1-containing protein  
337 complexes using fluorescence anisotropy assays, in which the anisotropy increases of  
338 fluorescein-labeled RNA oligonucleotides following protein titration were fit to obtain the  
339 apparent equilibrium binding affinities (Supplemental Fig. S12; Supplemental Materials  
340 and Methods). The recombinant proteins comprised either WT or S34F-mutant U2AF1  
341 as ternary complexes with the U2AF2 and SF1 subunits that recognize the adjoining 3'

342 splice site consensus sequences. The constructs were nearly full length and included  
343 the relevant domains for 3' splice site recognition [15,25,26] (Fig. 5A). The six pairs of  
344 tested RNA oligonucleotides (33 - 35 nucleotides in length) were derived from the  
345 proximal or distal 3' splice sites of the six genes listed above (Figs. 5B, S12). Combined  
346 with prior results for sequence variants derived from the S34F-skipped *DEK* cassette  
347 exon [18], we have in total measured binding affinities for 16 RNA oligonucleotides,  
348 which consist of five sequences with a U at the -3 position of the 3' splice site ("UAG"  
349 splice sites), seven "CAG" splice sites, and four "AAG" splice sites.

350         The trends among S34F-altered RNA binding affinities of U2AF1 complexes (Fig.  
351 5C - H) for the tested splice site sequences generally agreed with the nucleotide  
352 distributions observed in consensus 3' splice site that are promoted or repressed by  
353 *U2AF1S34F* (Figs. 1A, S1A). The S34F mutation reduced the affinities of U2AF1-  
354 containing complexes for four out of five tested "UAG" splice sites, consistent with T as  
355 the most common nucleotide at the -3 position of the 3' splice site (henceforth referred  
356 to as -3T) for S34F-repressed exons. Likewise, the S34F mutation often increased the  
357 affinities of U2AF1 complexes for "CAG" splice sites (for three out of seven tested  
358 sequences), consistent with -3C as the most common nucleotide preceding S34F-  
359 promoted exons. The remaining tested "UAG" or "CAG" splice sites showed no  
360 significant difference between S34F and WT protein binding. The "AAG" splice sites  
361 lacked a consistent relationship to the S34F-induced RNA affinity changes of U2AF1  
362 complexes *per se*. However, the S34F mutation increased the binding of the U2AF1-  
363 containing complex for one "AAG" splice site for an S34F-promoted exon (*ZFAND1*),

364 which is consistent with the greater prevalence of -3A than -3T preceding S34F-  
365 promoted exons.

366 Overall, the altered binding affinities of U2AF1-containing complexes for the  
367 proximal 3' splice site could account for four of the six S34F-associated alternative  
368 splicing events (*CEP164*, *FMR1*, *ZFAND1*, *FXR1*) (Figs. 5C - F, Supplementary Table  
369 S3). Similar to the previously-tested S34F-skipped splice site in *DEK* [18], the S34F  
370 mutation decreased affinities of the U2AF1-containing complexes for the skipped 3'  
371 splice sites of the *CEP164* and *FMR1* exons (Fig. 5C, D). Remarkably, the S34F  
372 mutation enhanced binding of the U2AF1-containing complexes to the proximal 3' splice  
373 sites of *ZFAND1* and *FXR1* (Fig. 5E, F), which could explain the enhanced inclusion of  
374 these exons in cell lines and LUAD (Supplementary Table S3). In agreement with the  
375 observed splicing changes, the S34F mutation had no significant effect on the distal 3'  
376 splice sites of these exons.

377 The affinities of the mutant U2AF1 complexes for the proximal splice site  
378 oligonucleotides of the remaining two S34F-promoted exons (*ATR* and *MED15*) were  
379 either similar to wild-type or decreased (Fig. 5G, H). These results differed from the  
380 S34F-dependent increase in U2AF1 binding to the proximal 3' splice site that was  
381 observed for *ZFAND1* and *FXR1* (Fig. 5E, F), which could readily explain the enhanced  
382 exon inclusions. However, for the *ATR* pre-mRNA, the *U2AF1* mutation reduced binding  
383 to the distal more than to the proximal 3' splice site (Fig. 5G, third and fourth columns).  
384 Given co-transcriptional splicing in the 5'-to-3' direction, the downstream (as opposed to  
385 upstream) 3' splice sites could compete as splicing acceptors for a given 5' donor splice  
386 site when transcription is relatively rapid as compared to splicing. (Such 3' splice site

387 competition likely occurs relatively frequently, as the *ATR* cassette exon is alternatively  
388 spliced even in wild-type cells). As such, a “net gain” in affinity for the proximal relative  
389 to distal 3' splice site could explain the observed S34F-associated exon inclusion in  
390 *ATR* mRNAs. For the *MED15* pre-mRNA, deviation of the S34F-associated splicing  
391 changes and a simple RNA affinity model suggested that additional mechanisms control  
392 selection of the *MED15* 3' splice sites. In total, our measurements of *in vitro* RNA-  
393 binding affinities are sufficient to explain six of seven tested alterations in splice site  
394 recognition driven by *U2AF1S34F* (Fig 5C-H and in [18]).

395

396 **HBEC3kt and LUAD cells were not dependent on *U2AF1S34F* for growth, but wild-**  
397 **type *U2AF1* was absolutely required.**

398 Other than its effect on RNA splicing, the consequences of the *U2AF1S34F*  
399 mutation on cell behavior are largely unknown. Recurrent mutations, such as *U2AF1*  
400 *S34F*, are considered likely to confer a selective advantage to cells in which they occur  
401 when expressed at physiologically relevant levels. However, mutant HBEC3kt cells  
402 (MUT1a and MUT1b) do not exhibit obvious phenotypic properties of neoplastic  
403 transformation—such as a growth advantage over wild-type cells (Supplemental Fig.  
404 S13) or an ability to grow in an anchorage-independent manner—that are frequently  
405 observed in cultured cells expressing well-known oncogenes, like mutant *RAS* genes.

406 Another attribute of some well-known oncogenes, such as *BCR-ABL* fusion in  
407 chronic myeloid leukemia or mutant *EGFR* or *KRAS* in LUAD, is the dependence on  
408 sustained expression of those oncogenes for the maintenance of cell growth or viability.  
409 To determine whether LUAD cells harboring a pre-existing S34F mutation are

410 dependent upon (or “addicted to”) the mutant allele, we searched the COSMIC  
411 database for LUAD cell lines with the *U2AF1S34F* allele [27]. Two cell lines (H441 and  
412 HCC78) were found and both these cells exhibit copy number gains at the *U2AF1* locus  
413 (three copies for H441 cells; four copies for HCC78 cells) and one copy of a variant  
414 allele. We confirmed that *U2AF1S34F* was the minor allele in these cells by Sanger  
415 sequencing and allele-specific RT-qPCR (Supplemental Fig. S14A, B). We further used  
416 the CRISPR-Cas9 system to selectively disrupt the wild-type or mutant *U2AF1*  
417 sequences and then assessed the impact of inactivating the *U2AF1* alleles on the  
418 clonogenic growth of the two LUAD lines with the *U2AF1* mutation. In addition, we  
419 performed similar experiments with the LUAD cell line A549 (wild-type for *U2AF1*) and  
420 the HBEC3kt-derived MUT1a cell line.

421 In all instances, loss of the mutant allele did not impair cell growth. Only one line  
422 (H441) exhibited altered growth, in the form of a two-fold increase in clonogenicity (Fig.  
423 6A). Successful disruption of the *U2AF1S34F* allele was confirmed by restoration of a  
424 normal RNA splicing profile in subclonal cells derived from the clonogenic assay  
425 colonies (see Supplemental Figs. S14 – S17, Tables S4 and S5, and text below). In  
426 contrast, loss of the wild-type allele completely inhibited clonogenic growth in all tested  
427 cell lines, regardless of whether the line carried the *U2AF1S34F* allele or not. A rescue  
428 experiment confirmed that loss of cell growth was due to loss of wild-type *U2AF1*  
429 expression. The loss of clonogenic capacity after disrupting endogenous *U2AF1* in  
430 A549 cells was prevented by first transducing them with a form of wild-type *U2AF1*  
431 cDNA (Fig. 6B) that is not predicted to be a target for sgRNA-WT (Supplemental Fig.  
432 S8). Overall, these findings indicate that wild-type *U2AF1* is required for the clonogenic

433 growth of cells, including lung cancer cell lines, that the S34F mutant is unable to  
434 compensate for loss of the wild-type allele, and that LUAD cells with the S34F mutation  
435 are not dependent on the mutant allele for growth *in vitro*.

436 To examine the effect of *U2AF1*S34F on tumor growth *in vivo*, we derived H441  
437 and HCC78 cells transduced with Cas9 and sgRNA-S34F or sgRNA-GFP as polyclonal  
438 pools or as clones (Supplemental Figs. S14, S15). The cell lines were verified to either  
439 carry or not carry the *U2AF1*S34F allele, and we confirmed that the Cas9 and sgRNA-  
440 S34F-transduced cells lost the S34F-associated splicing program (Supplemental Figs.  
441 S16, S17).

442 We inoculated these subclonal cell lines subcutaneously in nude mice and  
443 monitored xenograft tumor growth. The H441-derived cell lines, in which the  
444 *U2AF1*S34F allele was disrupted, were able to establish tumors *in vivo* at rates similar  
445 to those observed for tumor cells carrying the mutant allele (Supplemental Table S6).  
446 The HCC78-derived cell lines did not grow palpable tumors after xenografting within the  
447 observation period, so the requirement for *U2AF1*S34F *in vivo* could not be tested in  
448 that line. These experiments show that *U2AF1*S34F is dispensable for growth of these  
449 LUAD cell lines *in vivo*, a result consistent with the clonogenicity assays shown in Fig. 6.  
450 We conclude that *U2AF1*S34F appears to be neither sufficient nor necessary for lung  
451 cell transformation in these assays. In contrast, wild-type *U2AF1* is required for cell  
452 viability, consistent with the retention of a wild-type allele in human cancers carrying  
453 common *U2AF1* mutations.

454  
455

## 456 **Discussion**

457           In this report, we have examined the mechanistic and phenotypic consequences  
458 of the common *U2AF1*S34F mutation. Our data demonstrate that the S34F:WT ratio  
459 controls the quantitative consequences of the *U2AF1* mutation for splice site  
460 recognition, and suggest that differential RNA-binding affinities of the mutant and wild-  
461 type protein result in preferential recognition of specific 3' splice sites. Moreover, our  
462 finding that wild-type *U2AF1* is required for cell survival irrespective of the presence or  
463 absence of *U2AF1*S34F explains the genetic observation that tumors always retain an  
464 expressed copy of the wild-type allele. Finally, we expect that the genetic models of  
465 *U2AF1*S34F that we derived from immortalized lung epithelial cells, as well as cell lines  
466 derived from lung adenocarcinomas with the mutation, will prove useful for future  
467 functional studies of this common mutation.

468

### 469 **The S34F:WT ratio controls S34F-associated splicing**

470           *U2AF1*S34F is known to induce specific splicing alterations, but it is not known  
471 how these changes are regulated. We show that the ratio of S34F:WT *U2AF1* gene  
472 products is a critical determinant of the magnitude of S34F-associated splicing. This  
473 conclusion was demonstrated in an isogenic lung epithelial cell line engineered to  
474 express *U2AF1*S34F from one of the two endogenous *U2AF1* loci, and was further  
475 supported by analyses of human LUAD transcriptomes carrying the *U2AF1*S34F allele.  
476 These results suggest that wild-type *U2AF1* antagonizes the splicing program  
477 associated with the S34F mutation.

478

479

## 480 **Altered RNA binding affinities often explain S34F-associated splicing changes**

481 We find that a major functional difference between purified S34F mutant and  
482 wild-type U2AF1 proteins resides in altered binding affinities for a subset of 3' splice  
483 sites. The trends in the RNA sequence preferences of S34F-mutant U2AF1 are  
484 consistent with the preferred 3' splice sites of S34F-affected transcripts (here and in [17-  
485 20,28]), which we use as the signature of S34F-associated differential splicing (Fig. 1A).  
486 For oligonucleotides that showed significant changes in binding affinities, the S34F  
487 mutation typically reduced or enhanced respective binding of the U2AF1 splicing factor  
488 complexes to 3' splice sites preceded by a -3U or -3C (Fig. 5 and [18]). In support of our  
489 findings for the relevant ternary complex of human U2AF1, U2AF2 and SF1 subunits,  
490 recent studies confirmed that the corresponding S34F mutation inhibited binding of the  
491 minimal fission yeast U2AF heterodimer to a "UAG" splice site RNA [21]. These S34F-  
492 altered RNA affinities are consistent with the location of the substituted amino acid in a  
493 zinc knuckle that may directly contact RNA [17]. Although the effects of the S34F  
494 mutation on binding 3' splice sites preceded by -3A are variable, extrusion or alternative  
495 U2AF1 binding sites for disfavored nucleotides could occur in different sequence  
496 contexts by analogy with other RNA binding proteins [29,30].

497 Several lines of evidence support the idea that U2AF1S34F is capable of  
498 initiating pre-mRNA splicing once it binds to RNA. Nuclear extracts of cells  
499 overexpressing mutant *U2AF1* can support *in vitro* splicing reactions more efficiently  
500 than nuclear extracts derived from cells overexpressing wild-type *U2AF1* for a minigene  
501 with a specific 3' splice site sequence [17]. In addition, mutant U2AF1 can compensate

502 for loss of the wild-type factor for the inclusion of some U2AF1-dependent cassette  
503 exons [31]. Our observations that the altered RNA-binding affinities correlate well with  
504 S34F-associated splicing for the majority of splice sites that we tested further suggest  
505 that mutant and wild-type U2AF1 are functionally equivalent for downstream steps of  
506 splicing (Fig. 5 and [18]).

507

### 508 **A working model of S34F-associated Splicing**

509 In light of our findings and existing evidence from the literature, we propose a  
510 model wherein mutant U2AF1 drives differential splicing by favoring the recognition of  
511 one of two competing 3' splice sites (Supplemental Fig. S18). This model is motivated  
512 by three key facts. First, alternative splicing, in contrast to constitutive splicing,  
513 necessarily results from implicit or explicit competition between splice sites. (For  
514 example, cassette exon recognition can involve competition between the 3' splice sites  
515 of the cassette exon itself and a downstream constitutive exon.) Second, mutant and  
516 wild-type U2AF1 complexes have different binding specificities, largely due to their  
517 preferences for distinct nucleotides at the -3 position, that lead them to preferentially  
518 bind distinct 3' splice sites. Third, mutant and wild-type U2AF1 are likely functionally  
519 equivalent once they bind to RNA. Therefore, altering the cellular ratio of mutant and  
520 wild-type U2AF1 changes the amount of total U2AF1 bound to a given 3' splice site in a  
521 sequence-specific manner, thereby promoting or repressing that splice site relative to a  
522 competing 3' splice site.

523 Our proposed model is not exclusive of other possible contributing effects, such  
524 as competitive binding of mutant and wild-type U2AF1 to a factor with low stoichiometry

525 (Supplemental Fig. S18), or effects of U2AF1S34F on the kinetics of co-transcriptional  
526 splicing as suggested recently [32]. Future studies are needed to resolve these  
527 possibilities.

528

### 529 **How are cells with the U2AF1 S34F mutation selected during oncogenesis?**

530 *U2AF1S34F* is recurrently found in LUAD, other solid tumors, and myeloid  
531 disorders, suggesting that the mutant allele confers a physiological property that  
532 provides a selective advantage during neoplasia. A gene ontology (GO) analysis for  
533 genes that show S34F-associated alternative splicing in HBEC3kt-derived isogenic cells  
534 shows significant alterations in many biological processes such as mRNA processing,  
535 RNA splicing, G2/M transition of mitotic cell cycle, double-strand break repair and  
536 organelle assembly (FDR-adjusted p-values < 0.001). However, we did not observe  
537 signs of neoplastic transformation or changes in cell proliferation after introducing  
538 *U2AF1S34F* into the endogenous *U2AF1* locus in HBEC3kt cells (Supplemental Fig.  
539 S13). Moreover, targeted inactivation of *U2AF1S34F* in LUAD cell lines does not  
540 diminish, and in one case even increases, clonogenic growth in culture (Fig. 6).

541 The lack of a testable cellular phenotype has been a major hindrance to  
542 understanding the functional significance of mutant *U2AF1* in carcinogenesis. Cell  
543 proliferation is only one of the many hallmarks of cancer, so careful examination of other  
544 cell properties in the isogenic cells may be needed to establish the presumptive role of  
545 *U2AF1S34F* in carcinogenesis.

546 More recently, after completion of our study [33], Park *et al* reported that  
547 tumorigenic cells emerge after *U2AF1S34F* is ectopically produced in Ba/F3 pro-B cells

548 or in an immortalized line of small airway epithelial cells [34]. The authors attributed the  
549 transformation events by mutant U2AF1 to the consequences of altered 3' processing of  
550 mRNA's. In particular, they observed an increase in the length of the 3' untranslated  
551 region of *ATG7* mRNA and a reduction in the amount of ATG7 protein, proposing that  
552 the anticipated defect in autophagy predisposes cells to mutations, some of which are  
553 transforming. This “hit-and-run” type of mechanism is consistent with our observation  
554 and theirs that mutant U2AF1 is dispensable for maintenance of the transformed  
555 phenotype in LUAD cell lines (Figure 6) and in their cell lines [34]. Their observations do  
556 not, moreover, exclude a role for S34F-associated splicing in the oncogenic  
557 mechanism.

558

### 559 **Can cancer cells carrying the S34F mutation be targeted therapeutically?**

560 We have shown that the wild-type *U2AF1* allele is absolutely required for the  
561 growth of lung epithelial and LUAD cells that carry a mutant *U2AF1* allele (Fig. 6). This  
562 result indicates that mutant U2AF1 cannot complement a deficiency of wild-type U2AF1;  
563 it may also explain why tumors homozygous for the *U2AF1*S34F mutation have not  
564 been observed, although the number of tumors found to have even a heterozygous  
565 mutation is still relatively small, so the analysis may not be adequately powered. Still,  
566 the frequent occurrence of a low ratio of S34F:WT *U2AF1* mRNA, accompanied by  
567 increased copy number of wild-type *U2AF1* alleles in lung adenocarcinoma cell lines  
568 and possibly LUADs, suggests that there may be selection for a lower ratio of S34F:WT  
569 in addition to the likely selection, perhaps at an earlier stage of tumorigenesis, for the  
570 S34F mutant.

571           These results are consistent with a study of mutations affecting the splicing factor  
572 SF3B1, which reported that cancer cells harboring recurrent *SF3B1* mutations also  
573 depend on wild-type SF3B1 for growth [35]. Finally, a recent study similarly found that a  
574 wild-type copy of *SRSF2* is required for leukemic cell survival, and that *SRSF2*  
575 mutations generated a therapeutic index for treatment with a small molecule that inhibits  
576 3' splice site recognition [36]. Together, our results and these recent studies provide a  
577 genetic rationale for targeting wild-type splicing factors (or the splicing machinery more  
578 generally) in cancers harboring spliceosomal mutations.

579 **Materials and Methods**

580 ***Cell culture, reagents, and assays***

581 The HBEC3kt cells (a gift from Dr. John Minna, UT Southwestern Medical  
582 Center), H441, A549 (ATCC) and HCC78 cells (DMSZ) were cultured as previously  
583 described [22] or according to vendors' instructions. The primary antibodies for  
584 immunoblots are: rabbit anti U2AF1 (1:5000, # NBP1-19121, Novus), rabbit anti GFP  
585 (1:5000, #A-11122, Invitrogen), mouse anti ACTB (1:5000, Clone 8H10D10, Cell  
586 Signaling). Lentiviruses were produced and titered in HEK293T cells as previously  
587 described [37]. An MOI (multiplicity of infection) of 1 – 5 were used for all assays.

588 Total RNA was extracted and reverse transcribed as previously described [38].  
589 Splicing alterations were measured by quantitative PCR on reverse-transcribed cDNA  
590 (RT-qPCR), using isoform-specific primers (Supplemental Table S7). These primers  
591 were designed following a previously described method [39]. The PCR efficiency and  
592 specificity of each primer set were determined before they were used for measuring  
593 splicing changes (See Supplemental Materials and Methods for details).

594 Clonogenic assay was performed by infecting cells with lentiviruses two days  
595 before seeding them into 100 mm dishes (1000 live cells per dish) to grow colonies.  
596 Growth media were supplemented with puromycin (1 µg/ml) for selecting infected cells  
597 and were changed once a week for up to three weeks. Cell colonies were stained with  
598 0.03% methylene blue (in 20% methanol) for 5 min. Clonogenicity is defined as colony  
599 numbers formed as a percent of those in control cells.

600           Details of all DNA constructs used in the study and the genome editing  
601 approaches for creating the *U2AF1*S34F allele and allelic-specific disruption of *U2AF1*  
602 are described in the Supplemental Materials and Methods.

603

#### 604 ***mRNA sequencing and analysis***

605           High throughput mRNA sequencing (RNA-seq) was conducted in the Sequencing  
606 Facility of the National Cancer Institute. RNA quality was assessed by 2100 Bioanalyzer  
607 (Agilent). Total RNA with good integrity values (RIN > 9.0) was used for poly A selection  
608 and library preparation using the Illumina TruSeq RNA library prep kit. Two or four  
609 samples were pooled per lane and ran on the HiSeq2000 or HiSeq2500 instrument  
610 using TruSeq V3 chemistry. All samples were sequenced to the depth of 100 million  
611 pair-end 101 bp reads per sample.

612           Splicing analysis of RNA-seq data from the TCGA LUAD cohort as well as  
613 engineered HBEC3kt, H441, and HCC78 cell lines was performed as previously  
614 described [17]. A brief description of the method was provided in the Supplemental  
615 Materials and Methods.

616

#### 617 ***Purification of U2AF1 protein complexes and RNA affinity measurement***

618           Purification of U2AF1 complexes, as illustrated in Fig.5, was explained in  
619 Supplemental Materials and Methods. Sequences of synthetic 5'-labeled fluorescein  
620 RNAs (GE Healthcare Dharmacon) and binding curves are given in the Supplementary  
621 Fig. S12. Apparent equilibrium affinity constant of the purified U2AF1 complexes with  
622 RNA was measured based on changes in fluorescence anisotropy as previously

623 described [18]. A brief description of this method was provided in the Supplemental  
624 Materials and Methods.

625

626 ***Statistics***

627 All experiments were independently performed at least three times unless  
628 otherwise stated. Statistical significance was determined by two-tailed Student's *t* test or  
629 otherwise stated. In all analyses, *p* values  $\leq 0.05$  are considered statistically significant.

630

631

632 **Acknowledgements**

633 We thank Ms. Jackie Idol, Ursula Harper, Danielle Miller-O'Mard and the  
634 transgenic mouse core at NHGRI for technical assistance, Dr. Heidi Dvinge (FHRCRC)  
635 for help with the LUAD data analysis, Dr. Matthew J. Walter (Wash.U.) for sharing the  
636 *CEP164* and *FMR1* splice site sequences prior to publication. We thank members of the  
637 Varmus lab, Drs. Janine Ilagan (FHRCRC) and Paul Liu (NHGRI) for helpful discussions  
638 during the course of the study. HV was supported by the Intramural Program at the  
639 National Institutes of Health and is now supported by the Meyer Cancer Center at Weill  
640 Cornell Medicine. RKB is supported by the Edward P. Evans Foundation, Ellison  
641 Medical Foundation (AG-NS-1030-13), NIH/NHLBI (R01 HL128239), and NIH/NIDDK  
642 (R01 DK103854). CLK is supported by the Edward P. Evans Foundation and  
643 NIH/NIGMS (R01 GM070503). The results published here are in part based upon data  
644 generated by the TCGA Research Network: <http://cancergenome.nih.gov/>.

645

646

647 **References**

- 648 1. Yoshida K, Sanada M, Shiraishi Y, Nowak D, Nagata Y, Yamamoto R, et al.  
649 Frequent pathway mutations of splicing machinery in myelodysplasia. *Nature*.  
650 2011;478: 64–69. doi:10.1038/nature10496
- 651 2. Graubert TA, Shen D, Ding L, Okeyo-Owuor T, Lunn CL, Shao J, et al. Recurrent  
652 mutations in the U2AF1 splicing factor in myelodysplastic syndromes. *Nature*  
653 *Genetics*. 2012;44: 53–57. doi:10.1038/ng.1031
- 654 3. Imielinski M, Berger AH, Hammerman PS, Hernandez B, Pugh TJ, Hodis E, et al.  
655 Mapping the hallmarks of lung adenocarcinoma with massively parallel  
656 sequencing. *Cell*. 2012;150: 1107–1120. doi:10.1016/j.cell.2012.08.029
- 657 4. Furney SJ, Pedersen M, Gentien D, Dumont AG, Rapinat A, Desjardins L, et al.  
658 SF3B1 Mutations Are Associated with Alternative Splicing in Uveal Melanoma.  
659 *Cancer Discovery*. 2013;3: 1122–1129. doi:10.1158/2159-8290.CD-13-0330
- 660 5. Wang L, Lawrence MS, Wan Y, Stojanov P, Sougnez C, Stevenson K, et al.  
661 SF3B1 and Other Novel Cancer Genes in Chronic Lymphocytic Leukemia. *N Engl*  
662 *J Med*. 2011;365: 2497–2506. doi:10.1056/NEJMoa1109016
- 663 6. Waterfall JJ, Arons E, Walker RL, Pineda M, Roth L, Killian JK, et al. High  
664 prevalence of MAP2K1 mutations in variant and IGHV4-34-expressing hairy-cell  
665 leukemias. *Nature Genetics*. 2014;46: 8–10. doi:10.1038/ng.2828
- 666 7. Cancer Genome Atlas Network. Comprehensive molecular portraits of human  
667 breast tumours. *Nature*. 2012;490: 61–70. doi:10.1038/nature11412
- 668 8. Biankin AV, Waddell N, Kassahn KS, Gingras M-C, Muthuswamy LB, Johns AL,  
669 et al. Pancreatic cancer genomes reveal aberrations in axon guidance pathway  
670 genes. *Nature*. 2012;491: 399–405. doi:10.1038/nature11547
- 671 9. Cancer Genome Atlas Research Network. Comprehensive molecular profiling of  
672 lung adenocarcinoma. *Nature*. 2014;511: 543–550. doi:10.1038/nature13385
- 673 10. Ruskin B, Zamore PD, Green MR. A factor, U2AF, is required for U2 snRNP  
674 binding and splicing complex assembly. *Cell*. 1988;52: 207–219.
- 675 11. Zamore PD, Green MR. Identification, purification, and biochemical  
676 characterization of U2 small nuclear ribonucleoprotein auxiliary factor. *Proc Natl*  
677 *Acad Sci U S A*. 1989;86: 9243–9247.
- 678 12. Krämer A, Utans U. Three protein factors (SF1, SF3 and U2AF) function in pre-  
679 splicing complex formation in addition to snRNPs. *The EMBO Journal*. 1991;10:  
680 1503–1509.
- 681 13. Berglund JA, Abovich N, Rosbash M. A cooperative interaction between U2AF65

- 682 and mBBP/SF1 facilitates branchpoint region recognition. *Genes & Development*.  
683 1998;12: 858–867.
- 684 14. Merendino L, Guth S, Bilbao D, Martínez C, Valcárcel J. Inhibition of msl-2  
685 splicing by Sex-lethal reveals interaction between U2AF35 and the 3' splice site  
686 AG. *Nature*. 1999;402: 838–841. doi:10.1038/45602
- 687 15. Wu S, Romfo CM, Nilsen TW, Green MR. Functional recognition of the 3' splice  
688 site AG by the splicing factor U2AF35. *Nature*. 1999;402: 832–835.  
689 doi:10.1038/45590
- 690 16. Zorio DA, Blumenthal T. Both subunits of U2AF recognize the 3' splice site in  
691 *Caenorhabditis elegans*. *Nature*. 1999;402: 835–838. doi:10.1038/45597
- 692 17. Ilagan JO, Ramakrishnan A, Hayes B, Murphy ME, Zebari AS, Bradley P, et al.  
693 U2AF1 mutations alter splice site recognition in hematological malignancies.  
694 *Genome Res*. 2015;25: 14–26. doi:10.1101/gr.181016.114
- 695 18. Okeyo-Owuor T, White BS, Chatrikhi R, Mohan DR, Kim S, Griffith M, et al.  
696 U2AF1 mutations alter sequence specificity of pre-mRNA binding and splicing.  
697 *Leukemia*. 2015;29: 909–917. doi:10.1038/leu.2014.303
- 698 19. Brooks AN, Choi PS, de Waal L, Sharifnia T, Imielinski M, Saksena G, et al. A  
699 Pan-Cancer Analysis of Transcriptome Changes Associated with Somatic  
700 Mutations in U2AF1 Reveals Commonly Altered Splicing Events. Ast G, editor.  
701 *PLoS ONE*. 2014;9: e87361. doi:10.1371/journal.pone.0087361.s008
- 702 20. Przychodzen B, Jerez A, Guinta K, Sekeres MA, Padgett R, Maciejewski JP, et al.  
703 Patterns of missplicing due to somatic U2AF1 mutations in myeloid neoplasms.  
704 *Blood*. 2013;122: 999–1006. doi:10.1182/blood-2013-01-480970
- 705 21. Yoshida H, Park S-Y, Oda T, Akiyoshi T, Sato M, Shirouzu M, et al. A novel 3'  
706 splice site recognition by the two zinc fingers in the U2AF small subunit. *Genes &*  
707 *Development*. 2015;29: 1649–1660. doi:10.1101/gad.267104.115
- 708 22. Ramirez RD, Sheridan S, Girard L, Sato M, Kim Y, Pollack J, et al.  
709 Immortalization of human bronchial epithelial cells in the absence of viral  
710 oncoproteins. *Cancer Res*. 2004;64: 9027–9034. doi:10.1158/0008-5472.CAN-04-  
711 3703
- 712 23. Yusa K. Seamless genome editing in human pluripotent stem cells using custom  
713 endonuclease-based gene targeting and the piggyBac transposon. *Nat Protoc*.  
714 2013;8: 2061–2078. doi:10.1038/nprot.2013.126
- 715 24. Kralovicova J, Vorechovsky I. Allele-specific recognition of the 3' splice site of *INS*  
716 intron 1. *Hum Genet*. 2010;128: 383–400. doi:10.1007/s00439-010-0860-1
- 717 25. Liu Z, Luyten I, Bottomley MJ, Messias AC, Houngninou-Molango S, Sprangers

- 718 R, et al. Structural basis for recognition of the intron branch site RNA by splicing  
719 factor 1. *Science*. 2001;294: 1098–1102. doi:10.1126/science.1064719
- 720 26. Agrawal AA, Salsi E, Chatrikhi R, Henderson S, Jenkins JL, Green MR, et al. An  
721 extended U2AF(65)-RNA-binding domain recognizes the 3' splice site signal. *Nat*  
722 *Commun*. 2016;7: 10950. doi:10.1038/ncomms10950
- 723 27. Forbes SA, Beare D, Gunasekaran P, Leung K, Bindal N, Boutselakis H, et al.  
724 COSMIC: exploring the world's knowledge of somatic mutations in human cancer.  
725 *Nucleic Acids Res*. 2015;43: D805–11. doi:10.1093/nar/gku1075
- 726 28. Shirai CL, Ley JN, White BS, Kim S, Tibbitts J, Shao J, et al. Mutant U2AF1  
727 Expression Alters Hematopoiesis and Pre-mRNA Splicing In Vivo. *Cancer Cell*.  
728 Elsevier Inc; 2015;27: 631–643. doi:10.1016/j.ccell.2015.04.008
- 729 29. Lu G, Hall TMT. Alternate modes of cognate RNA recognition by human PUMILIO  
730 proteins. *Structure*. 2011;19: 361–367. doi:10.1016/j.str.2010.12.019
- 731 30. Miller MT, Higgin JJ, Hall TMT. Basis of altered RNA-binding specificity by PUF  
732 proteins revealed by crystal structures of yeast Puf4p. *Nat Struct Mol Biol*.  
733 2008;15: 397–402. doi:10.1038/nsmb.1390
- 734 31. Shao C, Yang B, Wu T, Huang J, Tang P, Zhou Y, et al. Mechanisms for U2AF to  
735 define 3' splice sites and regulate alternative splicing in the human genome. *Nat*  
736 *Struct Mol Biol*. 2014;21: 997–1005. doi:10.1038/nsmb.2906
- 737 32. Coulon A, Ferguson ML, de Turris V, Palangat M, Chow CC, Larson DR. Kinetic  
738 competition during the transcription cycle results in stochastic RNA processing.  
739 *Elife*. 2014;3. doi:10.7554/eLife.03939
- 740 33. Fei DL, Motowski H, Chatrikhi R, Prasad S, Yu J, Gao S, et al. Wild-type U2AF1  
741 antagonizes the splicing program characteristic of U2AF1-mutant tumors and is  
742 required for cell survival. *bioRxiv*. 2016 Apr. doi:10.1101/048553
- 743 34. Park SM, Ou J, Chamberlain L, Simone TM, Yang H, Virbasius C-M, et al.  
744 U2AF35(S34F) Promotes Transformation by Directing Aberrant ATG7 Pre-mRNA  
745 3. *Mol Cell*. Elsevier Inc; 2016;: 1–34. doi:10.1016/j.molcel.2016.04.011
- 746 35. Zhou Q, Derti A, Ruddy D, Rakiec D, Kao I, Lira M, et al. A Chemical Genetics  
747 Approach for the Functional Assessment of Novel Cancer Genes. *Cancer Res*.  
748 2015;75: 1949–1958. doi:10.1158/0008-5472.CAN-14-2930
- 749 36. Lee SC-W, Dvinge H, Kim E, Cho H, Micol J-B, Chung YR, et al. Modulation of  
750 splicing catalysis for therapeutic targeting of leukemia with mutations in genes  
751 encoding spliceosomal proteins. *Nat Med*. 2016. doi:10.1038/nm.4097
- 752 37. Fei DL, Sanchez-Mejias A, Wang Z, Flaveny C, Long J, Singh S, et al. Hedgehog  
753 Signaling Regulates Bladder Cancer Growth and Tumorigenicity. *Cancer Res*.

- 754 2012;72: 4449–4458. doi:10.1158/0008-5472.CAN-11-4123
- 755 38. Fei DL, Li H, Kozul CD, Black KE, Singh S, Gosse JA, et al. Activation of  
756 Hedgehog signaling by the environmental toxicant arsenic may contribute to the  
757 etiology of arsenic-induced tumors. *Cancer Res.* 2010;70: 1981–1988.  
758 doi:10.1158/0008-5472.CAN-09-2898
- 759 39. Brosseau JP, Lucier JF, Lapointe E, Durand M, Gendron D, Gervais-Bird J, et al.  
760 High-throughput quantification of splicing isoforms. *RNA.* 2010;16: 442–449.  
761 doi:10.1261/rna.1877010
- 762
- 763

764 **Figure Legends**

765 **Fig. 1. S34F-associated splicing program correlates with S34F:WT mRNA ratios in**  
766 **LUAD.**

767 **(A).** Different consensus 3' splice site sequences preceding cassette exons for two  
768 representative LUADs with the S34F mutation computed from published TCGA  
769 transcriptomes. In both cases, changes in the use of cassette exons were determined  
770 by comparisons with an average transcriptome from LUADs without *U2AF1* mutations.  
771 Boxes highlight nucleotides found preferentially at the -3 position. The nucleotide  
772 frequencies preceding exons that are more often included or more often excluded in  
773 tumors with the S34F mutation differ from the genomic consensus in the tumor from  
774 patient #7903, which represent “typical S34F” consensus 3' splice sites, but not in the  
775 tumor from patient #7727, which represent “quasi-WT” consensus 3' splice sites.  
776 (Consensus 3' splice sites from transcriptomes of every S34F-mutant LUAD are  
777 presented in Supplemental Fig. S1.) The analysis was restricted to introns with  
778 canonical GT-AG U2-type splice sites. The invariable AG at the 3' splice site was not  
779 plotted to scale in order to highlight the consensus sequences at the -3 position. The  
780 vertical axis represents the information content in bits (the maximal value is two. Zero to  
781 one bit is shown). *n* is the number of cassette exon sequences used to construct the  
782 logo. A cartoon illustrating alternative splicing of a cassette exon (black box) is shown  
783 on the left side of the sequence logo. Black lines over splice junctions illustrate the  
784 S34F-promoted isoform for each comparison. **(B).** *U2AF1*-mutant LUAD transcriptomes  
785 harboring “typical S34F” consensus 3' splice sites have relatively high S34F:WT mRNA  
786 ratios. *U2AF1*-mutant LUAD samples were grouped based on the nature of the  
787 consensus 3' splice sites. The asterisk represents a statistically significant change by

788 Student's t test. **(C)**. S34F:WT *U2AF1* mRNA ratios do not correlate with tumor purity in  
789 LUAD tumors with the S34F mutation. Tumor purity is represented by the percent of  
790 tumor nuclei in each LUAD sample (derived from TCGA clinical data) and plotted  
791 against the S34F:WT mRNA ratios. **(D)**. Inclusion of the *STRAP* cassette exon  
792 correlates with the S34F:WT mRNA ratio. Same as Panel **C** but the S34F:WT mRNA  
793 ratio is plotted against the inclusion frequency for the *STRAP* cassette exon. The  
794 median inclusion level of the same cassette exon for all transcriptomes from tumors  
795 without a *U2AF1* mutation (S34F:WT mRNA ratio = zero) is shown as a triangle. *r*,  
796 Pearson's correlation coefficient. In panels B – D, circles represent samples with typical-  
797 S34F consensus 3' splice site sequences; squares represent samples with quasi-WT  
798 consensus 3' splice site sequences. Colors indicate *U2AF1* copy number status as  
799 calculated by GISTIC 2.0 (See details in the Supplemental Materials and Methods):  
800 black, diploid; blue, shallow deletion; red, gain.

801

802

803 **Fig. 2. Creation of isogenic lung cell lines that recapitulate features of S34F-**  
804 **associated splicing.**

805 **(A)**. Strategy to create a TCT to TIT point mutation (S34F) at the endogenous *U2AF1*  
806 locus in HBEC3kt cells. TALEN, transcription activator-like effector nuclease; E, exon;  
807 mE, mutant (S34F) exon; ITR, inverted terminal repeat; HA, homology arm. See Results  
808 and Supplemental Materials and Methods for details. **(B)**. MUT1a and MUT1b cells  
809 contain similar levels of mutant and wild-type *U2AF1* mRNA. The number of reads  
810 supporting mutant or wild-type *U2AF1* was obtained from RNA-seq, using poly(A)-

811 selected RNA from the four cell lines. **(C)**. The S34F-associated cassette exons in  
812 *ASUN* and *STRAP* mRNAs show decreased inclusion in MUT cell lines. (Top) Scheme  
813 of alternative splicing with a cassette exon (black box) to generate short and long  
814 isoforms in which the cassette exon is excluded or included. (Bottom) Alternative  
815 splicing of cassette exons in *ASUN* and *STRAP* mRNAs, measured by RT-qPCR using  
816 isoform-specific primers. The short/long isoform ratio in WT1 cells was arbitrarily set to  
817 1 for comparison. Asterisks represent statistical significant changes as compared to that  
818 in WT1 cells. Error bars represent s.e.m. (standard error of the mean) (n = 4). **(D)**. Heat  
819 map depicting the inclusion levels of all cassette exons that showed at least a 10%  
820 change in use among the cell lines. The dendrogram was constructed from an  
821 unsupervised cluster analysis. **(E)**. Sequence logos from 3' splice sites preceding  
822 cassette exons with altered inclusion in MUT1a cells display typical S34F consensus 3'  
823 splice sites. Logos were constructed as in Fig. 1A based on the transcriptome of MUT1a  
824 cells in comparison with that of WT1 cells. Other comparisons of transcriptomes from  
825 MUT and WT cell lines yielded similar sequence logos.

826

827 **Fig. 3. The ratio of S34F:WT U2AF1 gene products controls S34F-associated**  
828 **splicing in isogenic HBEC3kt cell lines.**

829 **(A)**. Reduction of both mutant and wild-type U2AF1 RNA and protein does not affect  
830 S34F-associated splicing. WT1 and MUT1a cells were transduced with shRNAs against  
831 *U2AF1* (shU2AF1#1 and #4) or two control shRNAs (shScbr, an scrambled shRNA;  
832 shGFP, an shRNA against *GFP*). Total RNA and protein were harvested 4 days later.  
833 The frequencies of incorporation of cassette exon sequences in *ASUN* and *STRAP*

834 mRNAs (top and middle panels) were determined by the relative short/long isoform  
835 ratios by RT-qPCR, as represented in Fig. 2C. Immunoblots for U2AF1 and ACTB in  
836 total cell lysates are shown in the bottom panel. Asterisks represent statistical significant  
837 changes as compared to shScbr-transduced condition in each cell line. Error bars  
838 represent s.e.m (n = 3). **(B)**. Overexpression of wild-type or mutant *U2AF1* to change  
839 S34F:WT ratios alters S34F-sensitive splicing. WT1 and MUT1a cells were transduced  
840 with expression vectors encoding *GFP*, wild-type (WT) or mutant (S34F) *U2AF1* for 3  
841 days before harvesting cells to quantify the level of splicing changes and proteins as in  
842 panel A. Asterisks represent statistical significant changes as compared to GFP-  
843 transduced condition in each cell line. Error bars represent s.e.m (n = 3). **(C)**. Disruption  
844 of WT *U2AF1* by gene editing to increase S34F:WT ratios enhances S34F-sensitive  
845 splicing. WT1 and MUT1a cells were transduced with Cas9 and either sgRNA-GFP or  
846 sgRNA-WT. Total RNA and protein were harvested 6 days later for assays as in panel  
847 **A**. Asterisks represent statistical significant changes as compared to Cas9 and sgRNA-  
848 GFP-transduced condition in each cell line. Error bars represent s.e.m. (n = 3).

849

850 **Fig. 4. Increasing the ratio of S34F:WT gene products by disrupting the wild-type**  
851 ***U2AF1* locus enhances S34F-associated splicing of cassette exons.**

852 **(A)**. RNA-seq was performed for WT1 and MUT1a cells transduced with Cas9 and  
853 either sgRNA-GFP or sgRNA-WT. Upper panel: The Venn diagrams show overlap of  
854 290 cassette exons that display at least a ten percent increase in inclusion levels in  
855 MUT1a cells relative to levels in WT1 cells, with or without CRISPR-Cas9-mediated  
856 disruption of wild-type *U2AF1*. Lower panel: Increasing the S34F:WT ratio by disrupting

857 wild-type *U2AF1* enhances the magnitude of S34F-associated splicing. The “waterfall”  
858 plot depicts changes in percent inclusion levels for all shared cassette exons identified  
859 from the Venn diagram when the wild-type *U2AF1* locus was disrupted. Each vertical  
860 bar represents one shared cassette exon. **(B)**. The analysis shown in Panel A was  
861 repeated for cassette exons showing ten percent or more decreased inclusion in  
862 MUT1a cells. **(C)**. Heat map depicting the inclusion levels of all cassette exons that  
863 showed at least a 10% change in use among the treatment conditions. The dendrogram  
864 was constructed from an unsupervised cluster analysis. **(D)**. Enhanced features of  
865 S34F-associated logos at 3' splice acceptor sites after disruption of wild-type *U2AF1*.  
866 Sequence logos were constructed as in Fig. 1A, based on the indicated comparisons.  
867

868 **Fig. 5. Differential binding of mutant and wild-type U2AF1 complexes to RNA**  
869 **oligonucleotides explains most S34F-associated alterations in RNA splicing.**

870 **(A)**. Cartoons illustrate components of recombinant U2AF1 complexes used in the  
871 binding assay. Full-length proteins are shown but only partial sequences (denoted by bi-  
872 directional arrows) were used to make recombinant protein complexes. KH-QUA2, K-  
873 Homology Quaking motif; RRM, RNA recognition motif domain; RS, arginine/serine-rich  
874 domain; UHM, U2AF homology motif; ULM, U2AF ligand motif; ZnF, zinc finger domain.  
875 **(B)**. Scheme of alternative splicing patterns for cassette exons (top diagram) and 5'  
876 extended exons from competing 3' splice site selection (bottom). The brackets indicate  
877 the positions of RNA oligonucleotides used for the binding assays. Exons are shown as  
878 boxes: white boxes indicate invariant exonic sequences and black boxes denote  
879 sequences that are incorporated into mRNA (exonic) only when the proximal 3' splice

880 sites are used. Introns are shown as solid lines. The grey lines represent possible  
881 splices. The names of characterized genes that conform to the patterns shown in the  
882 upper and lower cartoons are indicated. **(C - H)**. Mutant and wild-type U2AF1  
883 complexes have different affinities ( $K_A$ 's) for relevant 3' splice site oligonucleotides. To  
884 accomplish the binding assays, the wild-type or mutant U2AF1 protein complexes were  
885 titrated into 5' fluorescein-tagged RNA oligonucleotides over a range of concentrations  
886 as described in the Supplemental Materials and Methods. RNA sequences from -4 to +3  
887 relative to the 3' splice sites (vertical lines) in proximal and distal positions are shown.  
888 The nucleotide at the -3 position is bolded and underlined. Empty bars,  $K_A$  for WT  
889 U2AF1 complex; grey bar,  $K_A$  for mutant U2AF1 complex. For ease of comparison  
890 between the affinity binding results with S34F-associated splicing, S34F-promoted  
891 splices, as determined from RNA-seq data, are shown on top of each bar graph in black  
892 lines. The fitted binding curves, full oligonucleotide sequences, and apparent equilibrium  
893 dissociation constants are shown in Supplemental Fig. S12. The relative changes in  
894 affinity and use of proximal *versus* distal splice sites are summarized in Supplemental  
895 Table S3. The asterisk represents a statistically significant change by unpaired t-tests  
896 with Welch's correction. ns, not statistically significant.

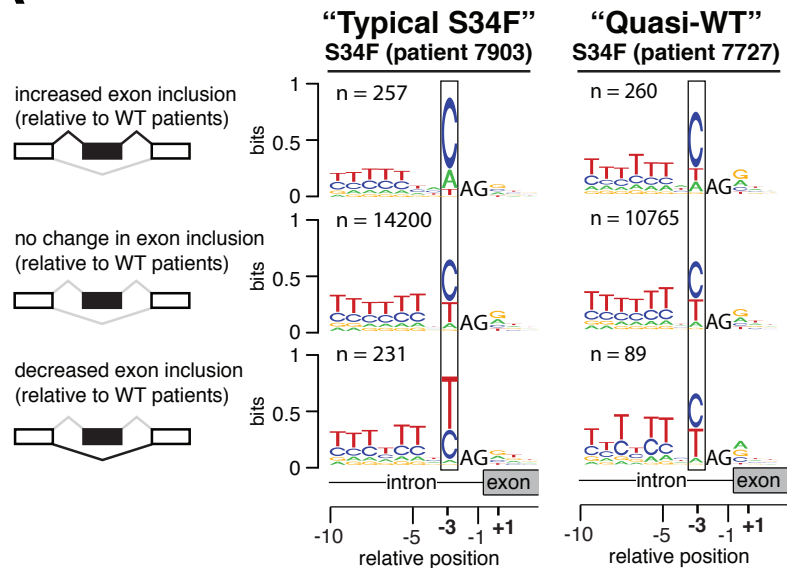
897

898 **Fig. 6. Wild-type but not mutant *U2AF1* is required for the clonogenic growth of**  
899 **the isogenic HBEC3kt cells and LUAD cell lines.**

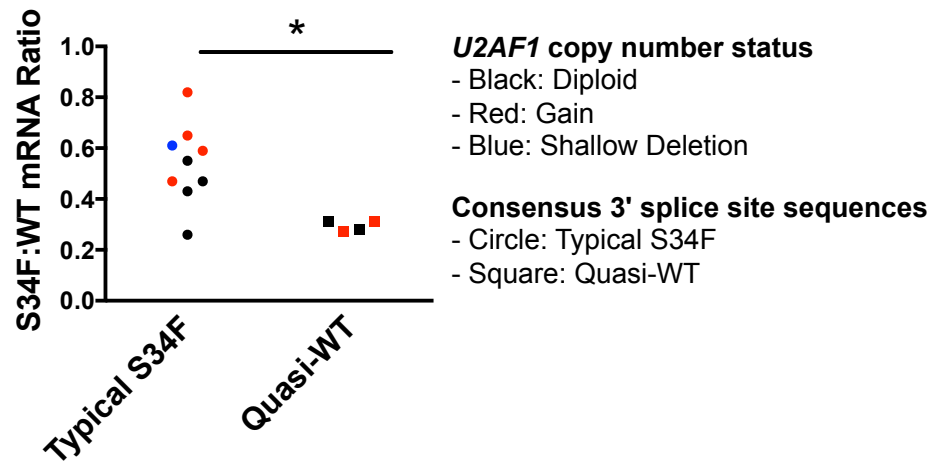
900 **(A).** Clonogenic growth assays after selective disruption of the wild-type or mutant  
901 *U2AF1* allele. Left panel: The indicated cell lines were transduced with lentiviruses  
902 expressing Cas9 and sgRNA-GFP, sgRNA-S34F or sgRNA-WT, followed by clonogenic

903 assays. Cell colonies were stained with methylene blue and counted three weeks later.  
904 Right panel: Quantification of the clonogenic assay. The results are shown as percent  
905 clonogenicity by setting the number of control cell colonies (cells transduced with Cas9  
906 and sgRNA-GFP) as 100%. Asterisks represent statistical significant changes as  
907 compared to Cas9 and sgRNA-GFP-transduced condition in each cell line. Error bars  
908 represent s.e.m (n = 3). **(B)**. Rescue of growth inhibition by Cas9 and sgRNA-WT by  
909 overexpressing a form of wild-type *U2AF1* cDNA that is not predicted to be the target for  
910 sgRNA-WT (See Supplemental Fig. S8 and Materials and Methods). Left panel: A549  
911 cells were transduced with a control (DsRed-Express 2) or a wild-type *U2AF1* cDNA  
912 that is not predicted to be the target for sgRNA-WT. Increased expression of wild-type  
913 *U2AF1* was confirmed by immunoblot (left bottom panel). These cells were  
914 subsequently transduced with Cas9 and either sgRNA-GFP or sgRNA-WT followed by  
915 clonogenic assays as in panel A (left upper panel). Right panel: Quantification as in  
916 Panel A. The asterisk represents a statistical significant change for the indicated  
917 comparison. Error bars represent s.e.m. (n = 3).  
918

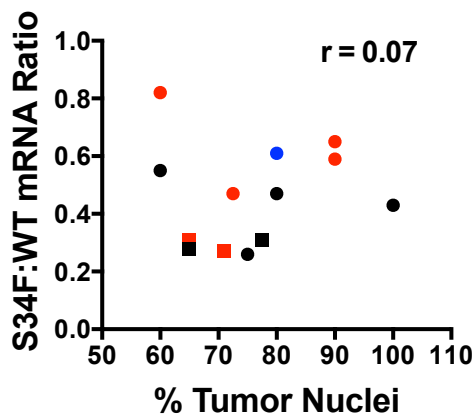
**A**



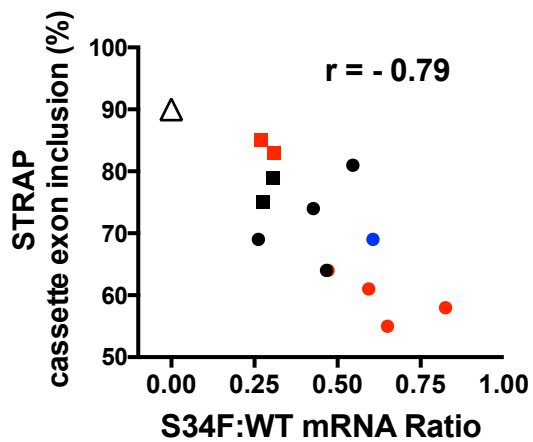
**B**

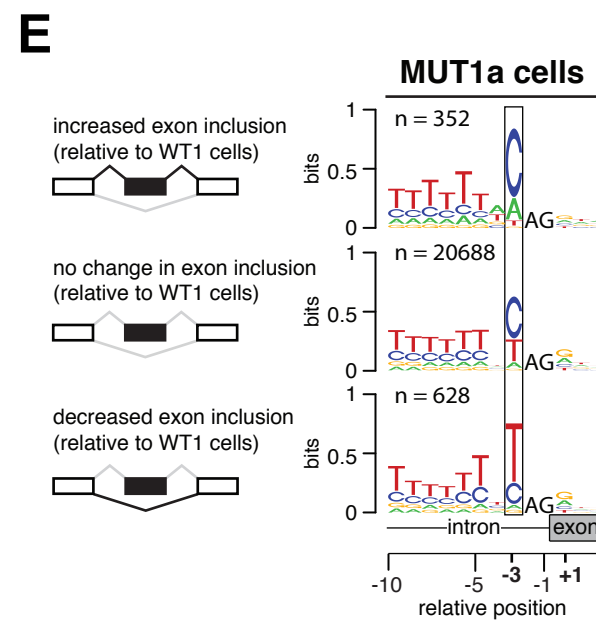
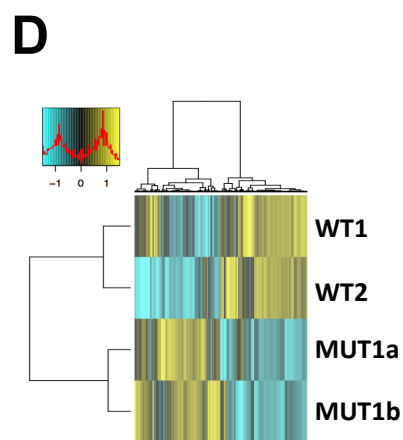
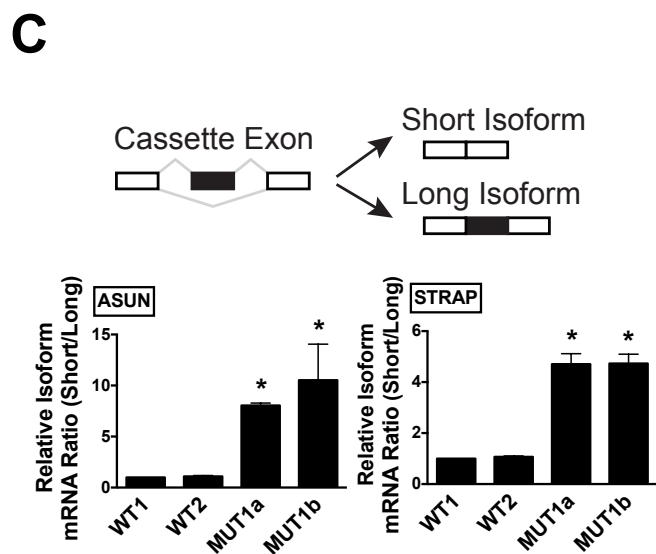
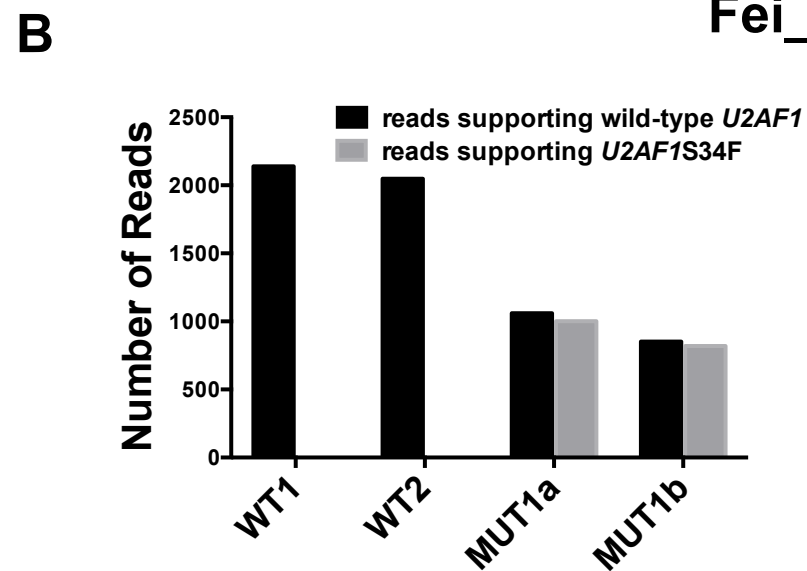
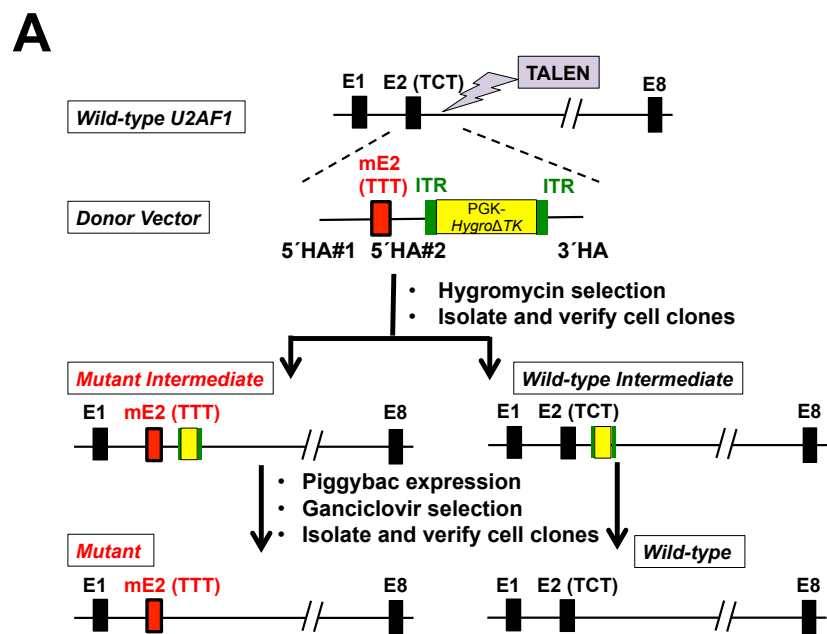


**C**



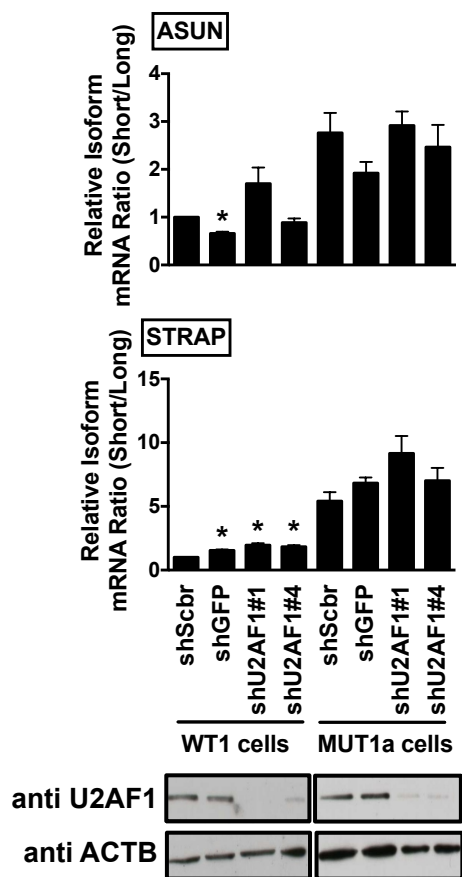
**D**





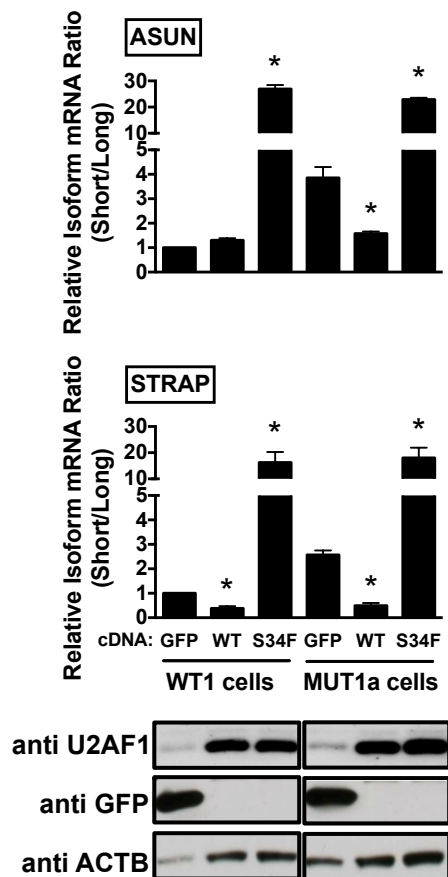
**A**

**Knockdown of total *U2AF1***



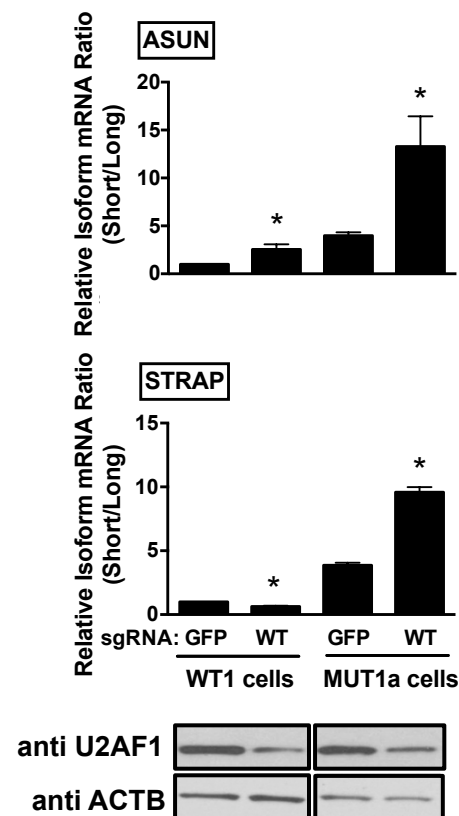
**B**

**Overexpression of WT or mutant *U2AF1***



**C**

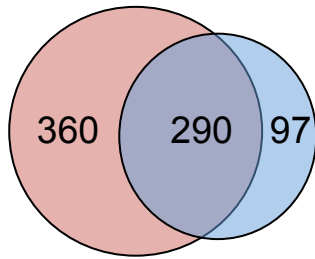
**Disruption of WT *U2AF1***



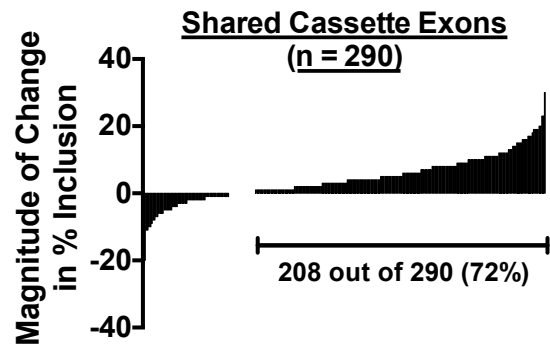
**A**

**Cassette Exons with Increased % Inclusion by *U2AF1S34F***

MUT1a cells  
sgRNA-WT  
vs.  
WT1 cells  
sgRNA-GFP  
(n = 650)



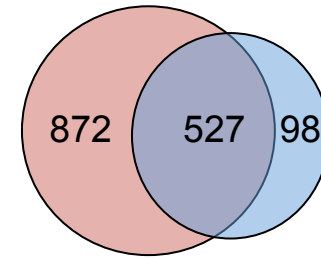
MUT1a cells  
sgRNA-GFP  
vs.  
WT1 cells  
sgRNA-GFP  
(n = 387)



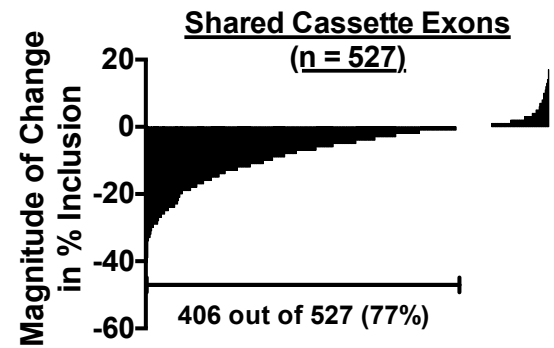
**B**

**Cassette Exons with Decreased % Inclusion by *U2AF1S34F***

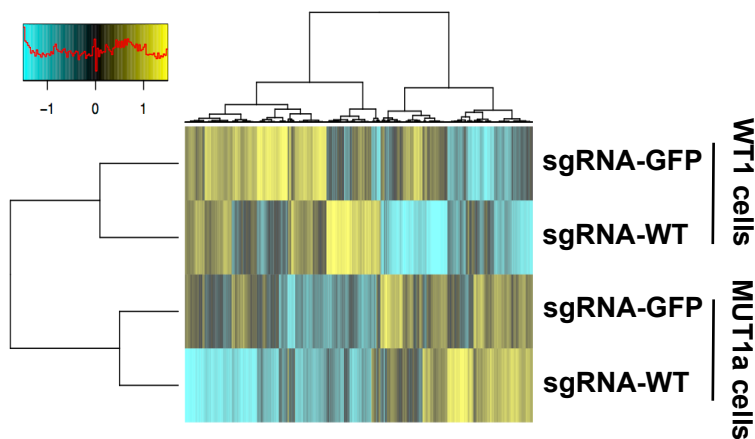
MUT1a cells  
sgRNA-WT  
vs.  
WT1 cells  
sgRNA-GFP  
(n = 1399)



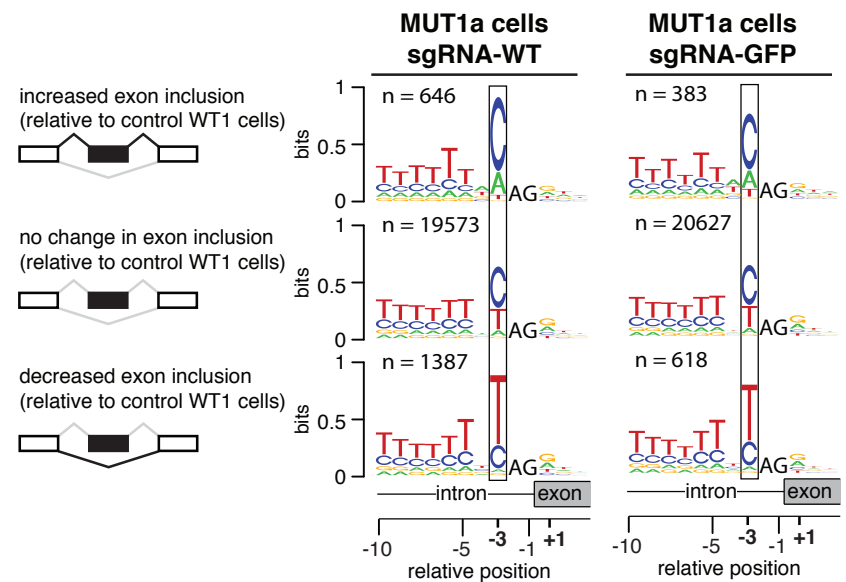
MUT1a cells  
sgRNA-GFP  
vs.  
WT1 cells  
sgRNA-GFP  
(n = 625)



**C**

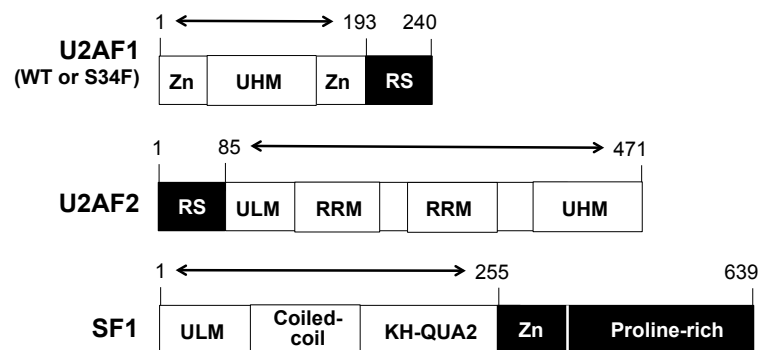


**D**

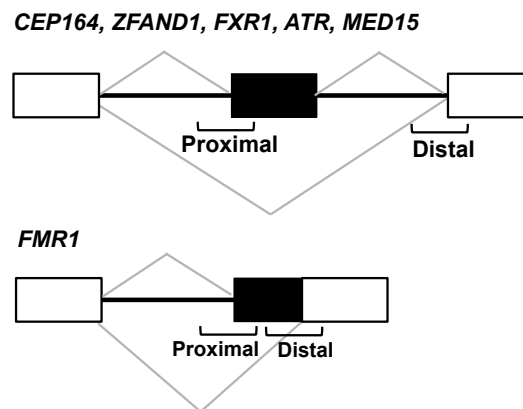


**A**

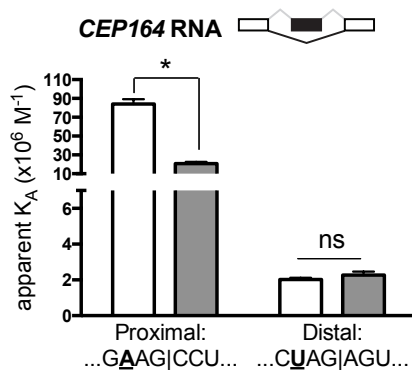
**Components of recombinant U2AF1 complex**



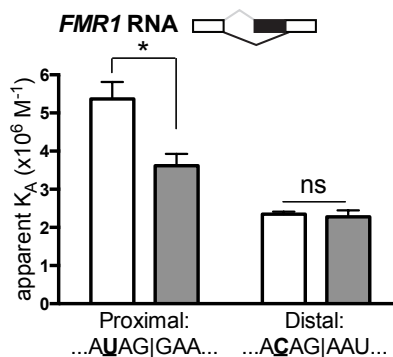
**B**



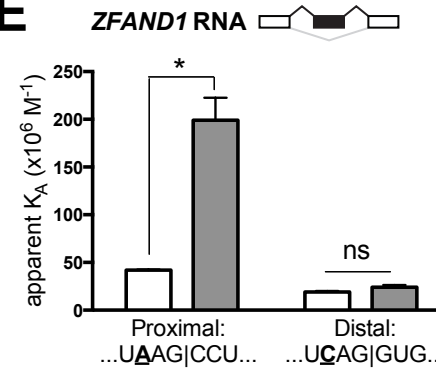
**C**



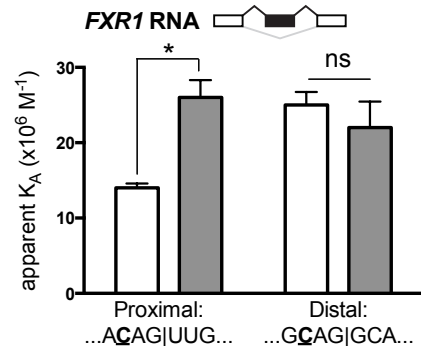
**D**



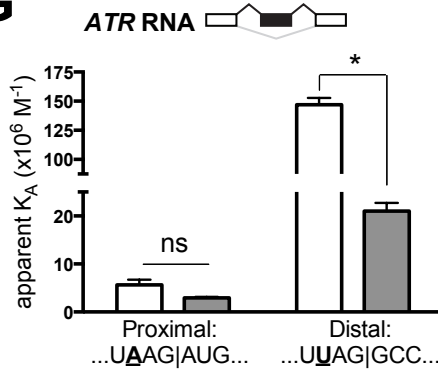
**E**



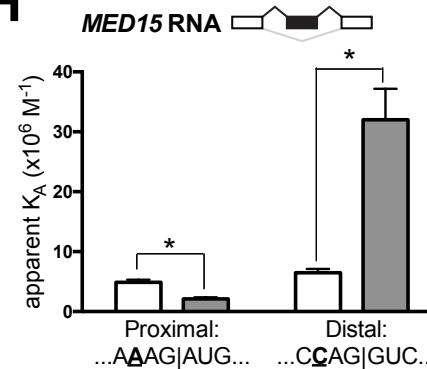
**F**



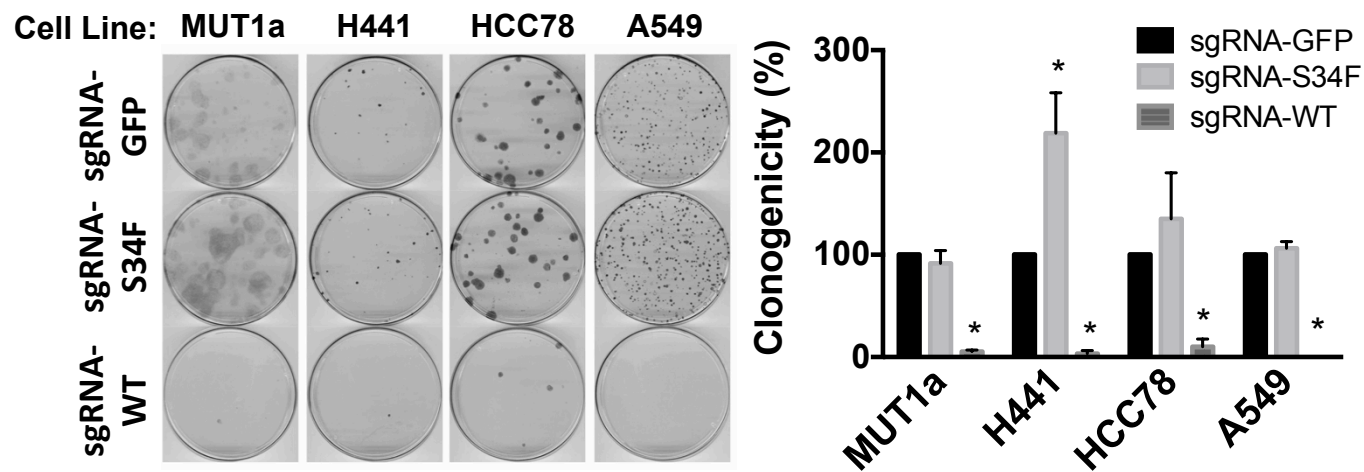
**G**



**H**



**A**



**B**

